Research Article

Microstructure, hardness and Tensile properties of Electron Beam Weld processed on Inconel-718 alloy

[1,*]Vishnu S, [2]Satheesh M, [3]Ramanan G

[1,*]Research Scholar, Department of Mechanical Engineering, Noorul Islam Centre for Higher Education, Kumaracoil, India-629180

[2]Department Mechanical Engineering, Noorul Islam Centre for Higher Education, Kumaracoil, India-629180

[3]Department Aeronautical Engineering, ACS College of Engineering, Bangalore, India-560074

***Email:** *vishnusanjiv@gmail.com*

Article History: Received: 11 January 2021; Revised: 12 February 2021; Accepted: 27 March 2021; Published online: 4 June 2021

Abstract:

Inconel 718 is the super alloy developed for elevated temperature service, usually based on group VIIIA elements, where relatively severe mechanical stressing is encountered, and high surface stability is frequently required. This paper presents the mechanical and metallurgical study of Electron Beam Welding process developed for Inconel 718 for an optimal parametric combination to yield favourable bead geometry and mechanical properties of welded joints. In the idea of observing the microstructures getting influenced by electron beam welding and thermal analysis, the plates of alloy that are hot-extruded have been butt welded by EBW at numerous speeds during welding. Outcomes illustrates that the alloy has been jointed defect less. The alloy is characterized by mechanical properties, SEM, XRD and TGA. On high range of welding speed, the NZ intensity at maximum range first goes down and then shoots up. In every scenario the alloys tensile properties after FSW goes down because of the region which softened at the heat-affected zone and some faithful conclusions are drawn.

Key words: Inconel-718; Electron Beam Welding; Hardness; Tensile; Bead Geometry, Microstructure.

1. INTRODUCTION

Electron Beam Welding (EBW) is a fusion welding process in which a beam of high-velocity electrons is focused on the materials to be joined. The work pieces melt as the kinetic energy of the electrons get transformed into heat upon impact. The technique is useful for the joining of Inconel 718 super alloy, with 50 - 55% Nickel as the main alloying element. Inconel – 718 finds extensive applications at high temperature regimes where retention of strength is of primary importance [1]. The super alloy has excellent creep-rupture strength at temperatures to 800^0C and finds application in gas turbines, rocket motors, spacecraft, nuclear reactors, pumps, and tooling. Good specific strength, high ductility, malleability and good corrosion resistance are other advantages. EBW is the preferred technology for joining Inconel alloy parts. It offers high power densities and allows joining of thick sections with very low heat input. Low heat input produces small Heat Affected Zones and Fusion Zones, and introduces relatively small distortions and thermal stresses which are one of the factors causing hot cracking phenomena during welding processes [2]. Additionally, low heat input minimizes Nb segregation and Laves formation which are undesirable phenomena as they increase Inconel 718 brittleness [3].

The Electron Beam Welding (EBW) process is mainly characterized by multiple process parameters such as welding current, focus current, welding speed, and accelerating voltage influencing multiple performance outputs such as bead geometry, mechanical metallurgical characteristics of weldment as well as the heat affected zone (HAZ), which subsequently affect overall weld quality [4]. Proper selection and control of process parameters can achieve satisfactory quality weld. However, EBW parameter optimization is very difficult due to existence of multiple quality indices which may be contradicting in nature depending on the requirements [5]. Moreover, direct and interactive effects of process parameters also influence extent of weld quality. It is therefore, quite essential to select the best suited process environment i.e. optimal parametric combination to produce desired quality weld [6].

Author exposed about effect of microstructural variations and tempted residual stresses on AZ31magnesium alloy joints tensile properties after EBW [7]. From the literature and the previous work done in the KL 134 Electron Beam Welding machine, among many independently controllable primary and secondary process parameters affecting the weld, the primary process parameters welding current, focus current, and welding speed were selected as process parameters for this study [8]. Acceleration voltage was kept constant at 60kV for all the trials. Consequently, this research targets principally on the special influence of EBW on microstructure, XRD, FT-IR, thermo gravimetric and mechanical properties of Inconel 718 alloy with similar speeds on welding involving specific attention was paid to examine the association connecting microstructure and mechanical properties of Inconel 718 alloy after EBW.

2. Materials and Methods

The Inconel-718 plates were cut into required sizes (100 mm X 80 mm X 6.6 mm) by Abrasive Water Jet Cutting machine. The chemical composition of the base metal is listed in Table 1. On holding rigidly the positioning of base materials over the anvil, but FSW process has been performed over the direction of extruding at a shoulder plunge depth of 0.15 mm, that has being set EBW machine, with a tool tilt angle of 2.5° [9]. Involving a greater choice of numerous pre-experiments, it has been finalized that rotation rate has to be approximately 1050 rpm to attain defect less weld joints holding outstanding exterior and mechanical properties by EBW, when welding speed was in a confident range [10, 11]. So the constant rotation rate was 1050 rpm. To examine the microstructure and properties of Inconel alloy after EBW at numerous welding speeds, whereas three dissimilar welding speeds have been utilized in this research [12]. The machine diagram of Inconel 718 alloy plates utilized for EBW is shown in Fig 1.

Table 1: Composition of Inconel - 718

Element	Weight %
Ni	50 - 55
Ti	0.65 – 1.15
Si	0.35 max
Cr	17.0 – 21.0 max
Al	0.2 – 0.8
P	0.015 max
Fe	Remainder
S	0.015 max
Nb	4.75 – 5.50
C	0.08 max
Mo	2.80 – 3.30 max
Mn	0.35 max
Cu	0.30 max
Co	1.0 max
B	0.006 max

Figure 1. Machine of Inconel 718 Alloy plates used for Electron beam welding

A large number of trial runs were carried out using 6.6 mm-thick plates of Inconel-718 to find out the feasible working limits of EBW process parameters. Different combinations of process parameters were used to carry out the trial runs [13]. This was carried out by varying one of the factors while keeping the rest of them at constant values. The working range of each process parameter was decided upon by inspecting the macrostructure (cross section of weld) for a smooth appearance without any visible defects such as large undercuts, underbead, incomplete fusion and spatter. The following observations were made from the trial run observations. When the weld current was lower than 60 mA, incomplete fusion of metals throughout the plate thickness was observed. It may be due to insufficient heat generation and insufficient metal transportation; on the other hand, when the weld current was higher than 80 mA, spatter and underbead was observed [14]. It may be due to the excessive turbulence caused by the vaporization of the metal. For finding the working limits of focus current, the beam was under focused, surface focused and over focused on the 6.6 mm thick Inconel-718 plate. The corresponding values of focus current were 525 mA, 530 mA and 535 mA. For speeds lower than 17 mm/s, and higher than 23 mm/s incomplete fusion was observed. Hence, the optimum value might be in this range. Joints Microstructures has been perceived by an optical microscope and a scanning electron microscope (SEM) at 20 kV with INCA Energy 350 energy-dispersive X-ray spectroscopy (EDS) analysis system. Once fragmented to little pieces and place it in a crucible, the sample's thermal analysis has been performed at a heating rate of 10 °C/min and an argon flow rate of 50 ml/min by utilizing differential scanning calorimetric [8]. On successful completion after grinding of samples utilizing silicon papers, phase composition and crystallographic texture distribution from the surface's top surface that has been tested by X-ray diffractometer (XRD) using Cu Kα radiation at 60 kV and 30 mA with a tilt angle of sample in the range from 10 to 90°.

In transverse direction, Hardness has been measured over the centre of the joint transversely over the mid-thickness every 1 mm positioning with a 120 g load for 10 s on MH-3 Vickers hardness tester. Samples of Transverse tensile test have been cut perpendicularly to the direction of extrusion for the BM and the weld joints before and after annealing, and the region that has been welded was put in centre within the 50 mm gauge length, implying with ASTM standard [12]. Tensile tests have been performed over a CMT-5105 mechanical tester with a crosshead speed of 0.5 mm/min at room temperature. Outcomes of tensile tests have been grabbed off from specimens that count three in safeguarding investigational outcomes accuracy and reliability. Table 2 shows the shows the selected design matrix based on Taguchi L27 orthogonal array consisting of 27 sets of coded conditions and the experimental results for the responses of Bead Width (BW) and Depth of Penetration (DP). All these data have been utilized for analysis and evaluation of optimal parameter combination required to achieve desired quality weld in terms of bead geometry within the experimental domain.

Table 2: Taguchi's Orthogonal Array L_{27} with responses

Run	Process			Experimental	
	Iw	If	S	BW	DP

1	1	1	1	4.196	6.525
2	1	1	2	4.453	6.410
3	1	1	3	5.215	6.565
4	1	2	1	4.443	7.295
5	1	2	2	4.591	6.541
6	1	2	3	4.343	6.435
7	1	3	1	4.895	7.624
8	1	3	2	4.613	7.753
9	1	3	3	5.013	8.612
10	2	1	1	6.593	7.795
11	2	1	2	5.583	7.698
12	2	1	3	5.101	6.321
13	2	2	1	5.565	7.250
14	2	2	2	5.291	7.255
15	2	2	3	5.761	7.364
16	2	3	1	5.014	7.056
17	2	3	2	4.816	6.953
18	2	3	3	5.123	7.395
19	3	1	1	5.531	8.050
20	3	1	2	5.063	7.568
21	3	1	3	5.271	7.885
22	3	2	1	5.325	7.400
23	3	2	2	5.675	7.001
24	3	2	3	5.270	6.786
25	3	3	1	5.151	6.914
26	3	3	2	5.431	6.854
27	3	3	3	5.050	7.006

3. Results and Discussion

3.1. Mechanical Properties

Distribution on hardness through the joint centre measured laterally with the mid-thickness is illustrated in Fig. 2. BM hardness tends to be in choice of 60–73 HV. It has been identified that the hardness distribution profiles showed subsequently to EBW. The profile hardness exposes minor disparity with collective welding speed. Hardness values at lower range have been experimental in the HAZ at irrespective of welding speed [13].

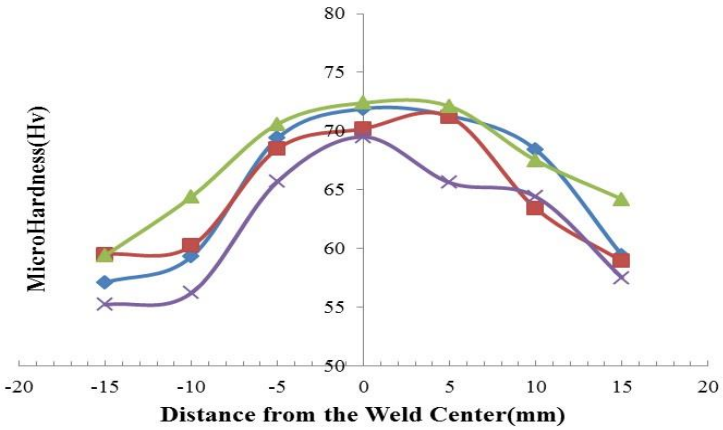

Figure 2. Hardness Properties of EBW Processed Inconel 718 alloy

The ultimate tensile strength (UTS), yield strength (YS) and elongation of the BM has been resolute to be about 852MPa and 28% correspondingly is illustrated in Fig.3. In plot it is notifying that the elastic behavior of the BM vs. weld joints has been dissimilar [7]. It has been noticed that after EBW decline in strength and elongation deprived of concern to welding speed, particularly the elongation. Both UTS and YS goes down with rise in welding speed has been noticed, though the cumulative degree of UTS was not much sure to YS. Joints elongation after EBW had unnoticeable variations with rising welding speed. The characteristic SEM micrographs of tensile fracture surfaces for the BM and the 120 mm/min joint are illustrated in Fig. 3. For the BM, the tensile fracture is inclusive of elongated dimples escorted by certain tear ridges, as illustrated in Fig. Also, the dimple-like features is illustrated on the surface of fracture of the weld joints after EBW.

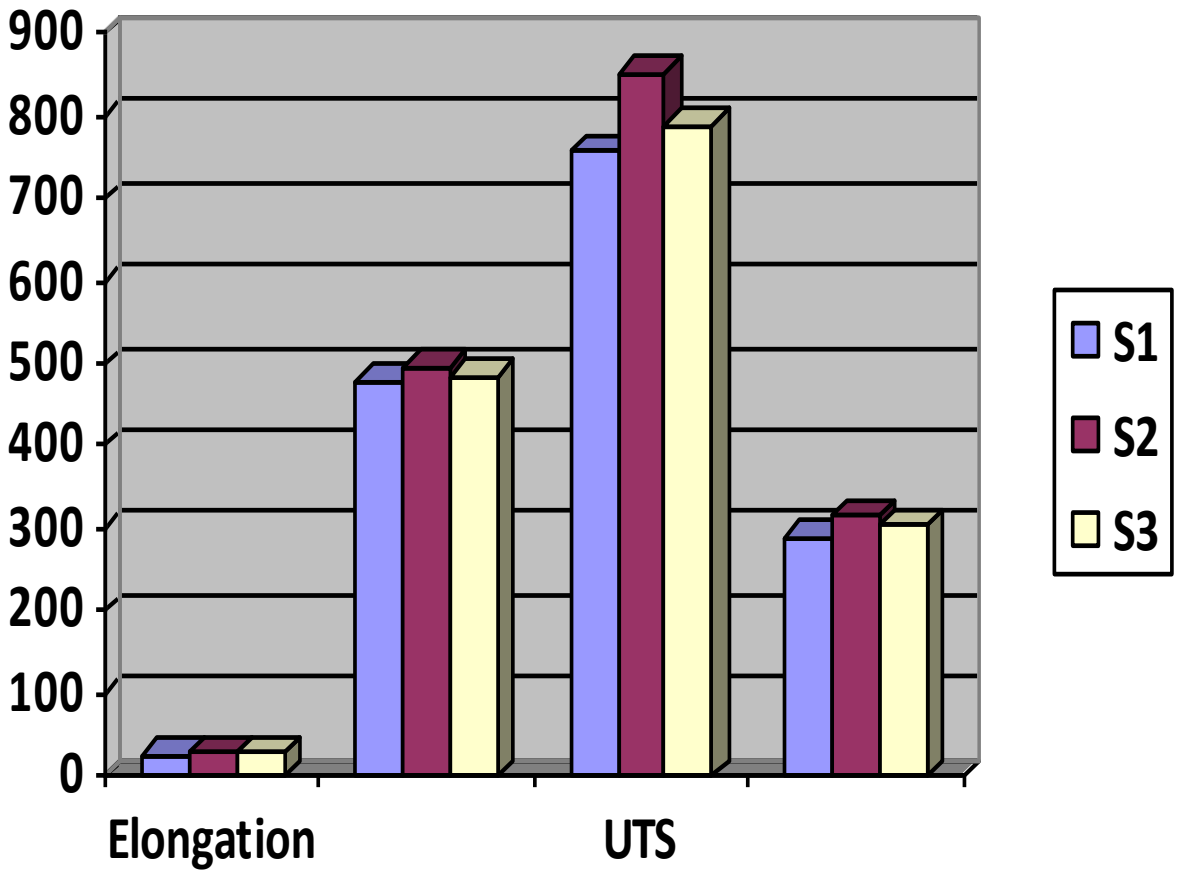

Figure 3. Histogram Image of Tensile Properties of the Inconel 718 Alloy

3.2. Microstructure

The SEM microstructures at dissimilar zones in the cross-section of the distinctive joints are illustrated in Fig. 4. The XRD analysis of the 718 alloy is depicted in Fig. 5 correspondingly. Fig.5 reveals the XRD analysis of the NZ in the joints after EBW [12]. Great range of peaks are identified with rapid rise of welding speed at a continuous rotation rate at high rpm, the grain size of Ni matrix diminished, though few intermetallic particles Zn scratched at the extraordinary welding speed. It discloses that Inconel 718 phase has been softened whereas base alloy phase persisted in the NZ of the welds after EBW that has been reliable with the XRD and SEM analysis [15].

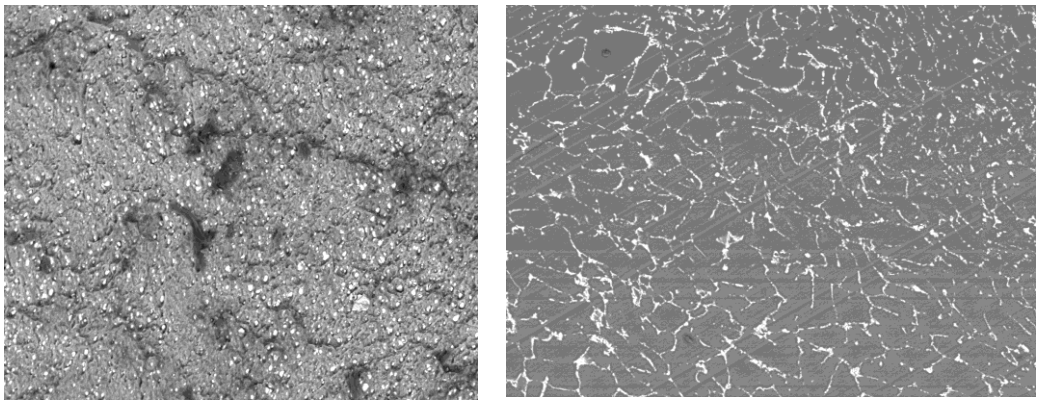

Figure 4. Microstructure of EBW processed Inconel 718 alloy at fracture zones

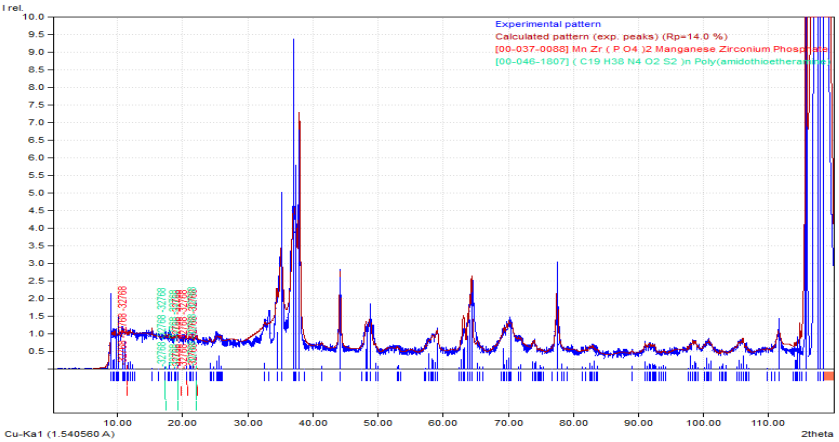

Figure 5. XRD analysis of EBW processed Inconel 718 alloy

3.3. Thermal Analysis

It is identified that the temperature associated to the peak attained while friction stir processing ranges between 650°C with translational speeds of 20–30 in/min at a constant rotation rate of 1050 rpm, and the peak temperature rises up with rise in rotation rate shown in Figure 6. Though alloy phase is with upright thermal stability, and its dissolution point is abundantly greater than the temperature of 800°C [19]. This takes place due to the reason that HAZ is heated adequately without plastic deformation of novel grains throughout FSW with cold work recovery and precipitates coarsening. The grains in the TMAZ are with convinced orientation in the metal-flow direction due to the stirring for the period of EBW.

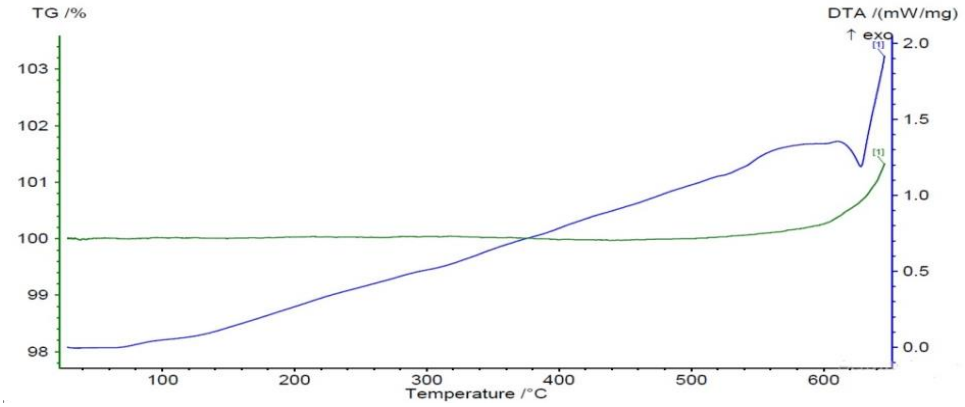

Figure 6. DSC heating temperature curves of EBW processed alloy at NZ

4. Conclusions

In the present work Inconel 718 alloy is welded by electron beam welding and the effects of on microstructure, XRD, DSC, hardness and Inconel 718 alloy tensile properties have been examined. Inconel 718 alloys has been joint quality is high at numerous welding speeds by EBW process. Joint that is welded shaped at 120mm/min gave a maximum ultimate tensile strength of 858MPa. The joints in tensile strength after EBW were lower than the BM strength that has been induced by the phase's dissolution in the nugget zone, the region that is softened at the heat-affected zone. XRD results confirm the existence of Ni and Zn alloy particles in the peak, with compounds has been found in the alloy. SEM images represents welding speed zone elements are consistently disseminated and the particles interfaces with one another are calculated. TGA/DTA illustrates that the rise in 5% of alloy inflated the amount of ignition. This absorption specifies within the chemical structure of the heat influenced zone at maximum rotational speed.

5. REFERENCES

1. Węglowski, M. S., Błacha, S., & Phillips, A. (2016). Electron beam welding–techniques and trends–review. Vacuum, 130, 72-92.
2. LIU, Y., GUO, Q., LI, C., MEI, Y., ZHOU, X., HUANG, Y., & LI, H. (2016). Recent progress on evolution of precipi-tates in inconel 718 superalloy. Acta Metall Sin, 52(10), 1259-1266.
3. Sharma, S. K., Agarwal, P., & Majumdar, J. D. (2017). Studies on electron beam welded inconel 718 similar joints. Procedia Manufacturing, 7, 654-659.
4. Sames, W. J., Medina, F., Peter, W. H., Babu, S. S., & Dehoff, R. R. (2014, November). Effect of process control and powder quality on Inconel 718 produced using electron beam melting. In 8th Int. Symp. Superalloy 718 Deriv (pp. 409-423).
5. Patel, V., Sali, A., Hyder, J., Corliss, M., Hyder, D., & Hung, W. (2020). Electron beam welding of inconel 718. Procedia Manufacturing, 48, 428-435.
6. Sames, W. J., Unocic, K. A., Dehoff, R. R., Lolla, T., & Babu, S. S. (2014). Thermal effects on microstructural heterogeneity of Inconel 718 materials fabricated by electron beam melting. Journal of materials research, 29(17), 1920-1930.
7. Li, Z., Chen, J., Sui, S., Zhong, C., Lu, X., & Lin, X. (2020). The microstructure evolution and tensile properties of Inconel 718 fabricated by high-deposition-rate laser directed energy deposition. Additive Manufacturing, 31, 100941.
8. Darwins, A. K., Satheesh, M., & Ramanan, G. (2018, August). Modelling and optimization of friction stir welding parameters of Mg-ZE42 alloy using grey relational analysis with entropy measurement. In IOP Conference Series: Materials Science and Engineering (Vol. 402, No. 1, p. 012162).
9. Ram, G. J., Reddy, A. V., Rao, K. P., Reddy, G. M., & Sundar, J. S. (2005). Microstructure and tensile properties of Inconel 718 pulsed Nd-YAG laser welds. Journal of Materials Processing Technology, 167(1), 73-82.
10. Raghavan, S., Zhang, B., Wang, P., Sun, C. N., Nai, M. L. S., Li, T., & Wei, J. (2017). Effect of different heat treatments on the microstructure and mechanical properties in selective laser melted INCONEL 718 alloy. Materials and Manufacturing Processes, 32(14), 1588-1595.
11. Deng, D., Moverare, J., Peng, R. L., & Söderberg, H. (2017). Microstructure and anisotropic mechanical properties of EBM manufactured Inconel 718 and effects of post heat treatments. Materials Science and Engineering: A, 693, 151-163.
12. Darwins, A. K., Satheesh, M., & Ramanan, G. (2018). Effect of thermo gravimetric and FTIR analysis on friction stir processed Mg–ZE42 alloy. Rasayan J Chem, 11(1), 365-371.
13. Reddy, G. M., Murthy, C. S., Rao, K. S., & Rao, K. P. (2009). Improvement of mechanical properties of Inconel 718 electron beam welds—influence of welding techniques and postweld heat treatment. The International Journal of Advanced Manufacturing Technology, 43(7), 671-680.

14. Sames, W. J., Unocic, K. A., Dehoff, R. R., Lolla, T., & Babu, S. S. (2014). Thermal effects on microstructural heterogeneity of Inconel 718 materials fabricated by electron beam melting. Journal of materials research, 29(17), 1920-1930.